AN ANALYSIS OF AC CIRCUITS AND ELECTROMAGNETISM

G. CHEN
Lab Technician, Data Analyst

L. CHEN
Lab Technician, Data Analyst, Notebook Author

E. SHEN
Lab Technician, Data Analyst,

K. WAN
Lab Technician, Data Analyst

U. YOUSAFZAI
Lab Technician, Data Analyst

(Received Dec. 18, 2019)

ABSTRACT

In this investigation, the properties of various AC circuits were measured in a variety of experiments using fundamental electronical components. The experimental properties measured were consistent with learned theory. For the constructed RC circuits, the residuals between the theoretical and experimental V-i phase shifts ranged from 0.017% to 0.200%. In the CLR circuit, the natural frequency was expected to be (2300±100)Hz. The frequency-potential amplitude graph was then regressed to find the natural frequency as the point where the potential is maximized. This was found to be (2460±30)Hz. The output potential of the constructed transformer was found to decrease significantly after an input frequency of approximately 29 kHz. A regression with R^2 value 0.98 was effected to describe the magnetic field as a function of distance along the longitudinal axis of the solenoid. The Biot-Savart Law was used to simulate the magnetic field that is produced by two off-axis solenoids.

I INTRODUCTION

Alternating current is the basis of the electrical grid system and modern electronics. By using basic equipment such as oscilloscopes and multimeters and learned theory, the properties of fundamental electrical components such as resistors, capacitors and inductors can be tested. Furthermore, the properties of electromagnetism were used to investigate the magnetic fields generated by solenoids.

II THEORY

The relationship between impedance, current, and potential is given by Ohm's Law:

$$V = iZ \qquad [1]$$

(C&J, 2001)

Where:
- i = Amplitude of current through a load
- V= Amplitude of potential across the load
- Z = The impedance

The reactance of a capacitor is given by

$$X_C = \frac{1}{2\pi f C} \qquad [2]$$

(HRW, 2010)

Where:
- X_C = Reactance of the circuit
- f = Frequency of AC source
- C = Capacitance of capacitor

The reactance of an inductor is given by

$$X_L = 2\pi f L \qquad [3]$$

(HRW, 2010)

Where:
- X_L = Reactance of the circuit
- f = Frequency of AC source
- L = Inductance of inductor

The impedance of an RC circuit is given by

$$Z = \sqrt{R^2 + X^2} \qquad [4]$$

(HRW, 2010)

Where:
Z = Impedance of circuit
R = Resistance of resistor

The phase angle of an RC circuit is given by

$$\phi = \tan^{-1}\left(\frac{X_C}{R}\right) \qquad [5]$$

(HRW, 2010)

Where:
ϕ = Phase angle of circuit

The natural frequency of an RCL circuit is given by

$$f = \frac{1}{2\pi\sqrt{LC}} \qquad [6]$$

(HRW, 2010)

The equation for the gain of a transformer is given as

$$V_S = V_P \frac{N_s}{N_P} \qquad [7]$$

(HRW, 2010)

Where:
V_p = Potential of primary coil
V_s = Potential of secondary coil
N_p = Number of turns of primary coil
N_s = Number of turns of secondary coil

The magnetic field generated by a current element is given by Biot-Savart Law:

$$d\vec{B} = \frac{\mu_0 i}{4\pi}\frac{d\vec{s} \times \vec{r}}{r^3} \qquad [8]$$

(HRW, 2010)

Where:
μ_0 = Permeability of free space
$d\vec{s}$ = Infinitesimal length current element
r = Distance from current element to where the magnetic field is computed

By effecting an integral of [8], the magnitude of the magnetic field induced by a solenoid can be determined to be,

$$\mathrm{B(z)} = \frac{\mu_0}{4\pi}\frac{iR^2}{2(R^2 + z^2)^{\frac{3}{2}}} \qquad [9]$$

(HRW, 2010)

Where:
R = Radius of solenoid
z = Distance from the closer end of the solenoid to probe

III METHOD

The RC circuit analysis was performed on a resistor with resistance 680 Ω and 1000 Ω and a capacitor with capacitance 1, 10, 47, and 220 μF, connected in series to a 4011A 5MHz function generator. The frequency produced for most of the circuits was (711.1±.2) Hz. The potential across the power source and the resistor was measured with a Tektronix TBS1052B oscilloscope. The corresponding Lissajous figures were constructed and analyzed.

The CLR circuit analysis was performed on a circuit constructed with a capacitor, a resistor, and an inductor connected in series to the function generator. The capacitance chosen for the frequency-amplitude analysis was (47±5) nF. The inductor had inductance (0.10±.01) H, and the resistor had resistance (2200±200) Ω. The oscilloscope measured potential across the source and the resistor. The corresponding frequency-amplitude graph was constructed and analyzed.

The transformer experiment was performed with two solenoids. The input solenoid was connected to the function generator and a metal core extended it to the output solenoid. The oscilloscope measured potential across the source and the output solenoid. The gain-frequency data was graphed and regressed sinusoidally using Python to find the frequency and amplitude of each run and then analyzed collectively.

The solenoid experiment was performed using a Helmholtz coil energized by a battery. The orientation of the Vernier B-field sensor that would yield the largest magnetic field reading was used. The sensor was mounted

onto a platform that was slid along the longitudinal axis of the solenoid. The position of the platform was recorded using a Vernier motion detector. The magnetic field over position graphs were analyzed.

IV Data

The data for the RC circuit, the CLR circuit, and the transformers was collected using the oscilloscope.

The battery used in the solenoid experiment was measured to have a voltage of (1.27±.05) V. The Helmholtz coil had 23 loops of wire, a diameter of (12.2±.2) cm, and a thickness of (1.85±.04) cm. The solenoid had a resistance of (1.6±.1) Ω.

V Analysis

The theoretical phase shift of the RC circuit is calculated using [5]. The Lissajous figures for each circuit was plotted, and the phase shift was calculated using the y-intercepts and maximum y values.

To ensure that the impedance of the function generator matched the impedance of the circuit, the impedance for the circuit was calculated prior to the empirical phase of this endeavor. The values of the phase shift were calculated as well, to determine if the phase shift would be visible in the Lissajous figure. The values ranged from (18.2 ± .3)° using a 1 μF capacitor and 680 Ω resistor to (0.1 ± .1)° using a 220 μF capacitor and 1000 Ω resistor.

To determine the accuracy of calculating phase shift using a Lissajous figure, the experimental values are compared to the theoretical values calculated using [5] and the residuals were calculated.

The residuals are all less than 1%, showing that the method used to calculate the phase shift of the Lissajous figure matches with the corresponding theory. As well as this, the Lissajous figure was also used to verify that the frequency of the source and the frequency of the circuit at equilibrium was indeed equal. This demonstrates the two common uses of Lissajous figures: to determine relative frequencies and to determine the phase shift between two signals.

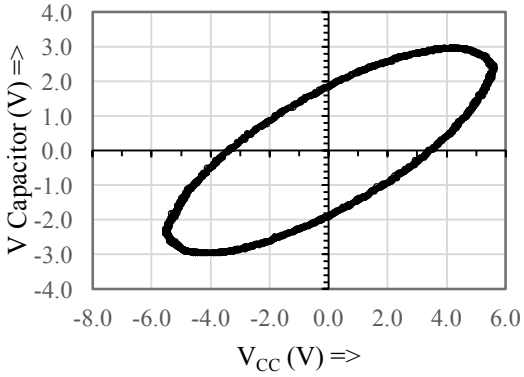

Fig 1. Lissajous figure of circuit with 1000 Ω resistor, 1μF capacitor, and frequency of 711.112 Hz. The vertical axis plots the potential across the capacitor as a function of time. The horizontal axis plots the signal as a function of time.

Index	Theoretical Phase Shift (degrees)	Empirical Phase Shift (degrees)	Residuals (%)
1	18.2±.3	18.5±.5	0.017
2	1.8±.4	1.5±.3	0.200
3	0.4±.2	0.4±.2	0.000
4	0.1±.1	0.1±.2	0.000
5	12.6±.5	13.8±.8	0.095
6	1.2±.3	2.0±.4	0.667
7	0.6±.2	0.5±.3	0.200

Fig 2. O-C table comparing the theoretical and empirical phase shifts and their respective residues. The theoretical values are calculated using reactance theory. The empirical values are calculated using Lissajous figures.

For the CLR circuit, the natural frequency of the circuit was first predicted with [6] to be (2300±100)Hz.

A range of values for the frequencies "around" the predicted natural frequency was then used and the amplitude of the potential across the resistor (which is a measure of the current throughout the circuit) was measured for each circuit. It is important to note that the AC power supply was kept constant throughout the runs.

Using [1], [2], [3], and [4], the expected potential amplitude across the resistor when the frequency of the AC current is no longer at its natural frequency can be found to be written as

$$V_R = \frac{V}{\sqrt{1+(\frac{2\pi Lf}{R}-\frac{1}{2\pi RCf})^2}} \qquad [10]$$

The three constants were than regressed using Python and the following expression for the potential across the resister was found.

$$V_R = \frac{(2.664\pm.008)}{\sqrt{1+(((2.31\pm.02)E-4)f-\frac{(1400\pm10)}{f})^2}} \qquad [11]$$

The regression had an R^2 value in excess of 0.99. The regression was then plotted alongside the measured values, producing the following graph.

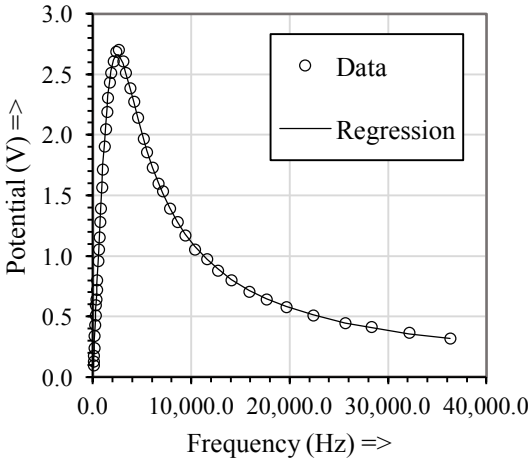

Fig 3. Graph of the amplitude of the potential across the resistor versus the frequency. The regression found earlier was plotted along side the data points, showing a near perfect fit.

Natural frequency occurs when the amplitude of the current (and thus V_R) is maximized. From [11], this obviously occurs when the denominator is equal to 1. Solving for this natural frequency yields (2460±30). Compared to the predicted natural frequency, a residual of around 7% was observed.

For the transformer experiment, the output potential began to drop after approximately 29kHz. A peak potential of approximately 5.2 V was recorded however using [7] the theoretical peak potential was found to be 4.7 V.

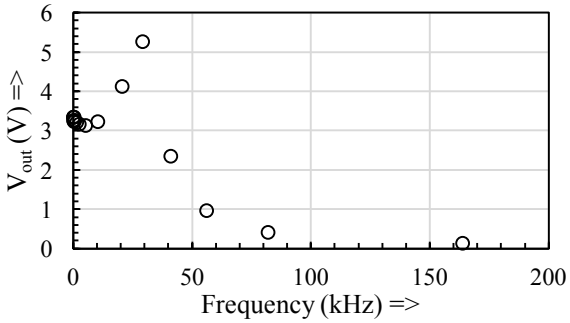

Fig 4. Graph of input frequency versus output potential of the transformer. A peak potential of 5.2 V can be observed at 29 kHz.

The decrease in potential is likely due to core losses and winding resistance. For core losses, the changing magnetic field not only induces current in the secondary coil but also in the iron core itself. These loops of current are called eddy currents and they cause heat loss known as Joule heating. Core losses also contain hysteresis losses in which the repeated core magnetizations by the alternating magnetic field allow for a small amount of energy to be lost as heat. This heat loss can be minimized by using a material that has a low hysteresis loss. Hysteresis loss is caused when the domains inside the core change alignment. Hysterics is the likeliest cause for the considerable drop in output potential as the frequency of the input voltage is increased. This is because for a given core material, the transformer energy loss due to hysterics is proportional to the input frequency and is a function of the peak flux density to which it is subjected to. Winding resistance occurs from current flowing through the primary and secondary windings resulting in Joule losses.

For the solenoid experiment, the data obtained from the magnetic field sensor was plotted against the motion detector data to obtain a graph of the magnetic field strength along the longitudinal axis of the solenoid.

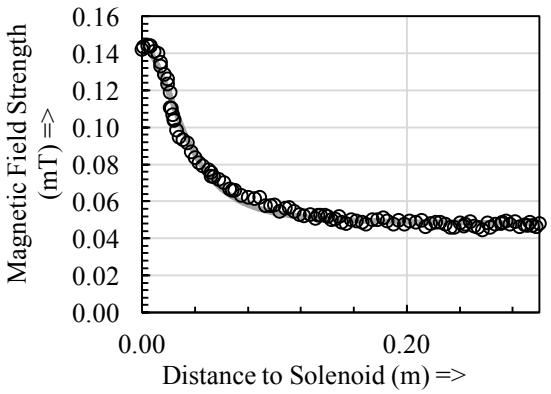

Fig 5. A plot of magnetic field strength over distance to the closer end of the solenoid with regression curve overlaid. The magnetic field appears to reach a horizontal asymptote at roughly 0.048 mT.

Equation [9] was converted to a more general form to allow the data to be regressed as:

$$B(z) = \frac{AB}{(B + z^2)^{\frac{3}{2}}} + C \qquad [12]$$

The extra constant was added to the regression to account for external magnetic fields including that of the Earth. This yields the equation:

$$B(z) = \frac{(1.76 \pm .03)E - 7}{((1.85 \pm .07)E - 3 + z^2)^{\frac{3}{2}}} + (4.81 \pm .02)E - 5 \qquad [13]$$

The regression had an R^2 value of 0.98. The constants obtained from the regression were then compared to the theoretical values to assess the validity of equation [9].

Constant	Experimental Value	Theoretical Value	Residuals (%)
A	(4.09±.03) E-6	(5.74±.02) E-6	28.7
B	(1.85±.07) E-3	(1.86±.03) E-3	0.5

Fig 6. O-C Table for the theoretical and experimental constants. The theoretical values were calculated using the measurements of the circuit elements and the experimental values were obtained from the regression. Large residuals were observed, likely due to the small quantities involved.

For the purpose of the simulation, a solenoid is approximated as a uniform helix structure.

For a solenoid aligned and centered on the x-axis that goes counter-clockwise in the +x-direction, we can thus describe it with the following parametric equation:

$$\vec{s} = (x_0 + hk, R\cos(2\pi nk), R\sin(2\pi nk)) \qquad [14]$$

Where:
x_0 = Initial x-position (m)
h = Thickness of solenoid
$0 \le k \le 1$ (the parametric variable)

From [14], we can also find that

$$\frac{d\vec{s}}{dk} = (h, -2\pi nR\sin(2\pi nk), 2\pi nR\cos(2\pi nk)) \qquad [15]$$

Integrating [8], and reformatting it, we can find that the magnetic field due to a single solenoid is

$$\vec{B}(\vec{v}) = \int_0^1 \frac{\mu_0 i}{4\pi} \frac{\frac{d\vec{s}}{dk} \times (\vec{v} - \vec{s}(k))}{|\vec{v} - \vec{s}(k)|^3} dk \qquad [16]$$

The simulation was first tested against the theoretical yields of the circuit used for the fourth experiment before adding in a second solenoid. The simulated values within the solenoid had average residuals of 2.87% compared with the theoretical values. This implies that the simulation should be valid. A second solenoid was added to the simulation at an angle of 73° to the first one. Effectively, the second solenoid was rotated about the z-axis, and thus has the parametric equations:

$$\vec{s} = R_{z\theta}\vec{s_1} \qquad [17]$$

$$\frac{d\vec{s}}{dk} = R_{z\theta}\frac{d\vec{s_1}}{dk} \qquad [18]$$

Where:
$R_{z\theta}$ = Rotation matrix about z-axis for an angle of θ
$\vec{s_1}$ is the parametric equation in [14].

In order to make a 3D plot of the magnetic field caused by these two solenoids,

an 11x11x11 mesh-grid of points nearby the two solenoids were chosen.

For each point on the grid, [16] was used with [14], [15], [17], and [18] to find the total magnetic field. For each point, [16] was used with the parametric equations of both solenoids to calculate the impact each one has on it. To find the total magnetic field, the two fields are superimposed and thus summed.

A plot of the magnetic field was produced by using an arrow at each of the 1331 reference points pointing in the direction of the magnetic field. Due to the high contrast of magnetic field strength, the square root of the magnitude of the field was taken to determine the length of the arrow to improve clarity.

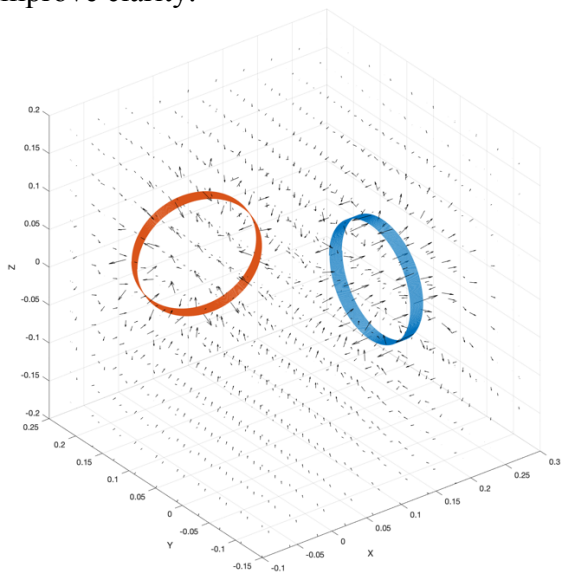

Fig 7. Vector field indicating the magnetic field lines around two solenoids. The solenoids are indicated with the red and blue rings. The vectors are scaled proportionally to the square root of the magnitude at the location.

VI Sources of Error

The capacitors and inductors used for the RC circuits had an uncertainty of 10%. Use of more reliable capacitors and inductors could have reduced the residuals for the time constants.

The oscilloscope was not precise enough as it depended on the pixels of the display, greatly affecting the data obtained from the circuits. This was especially evident in circuits with lower potentials as the rounding of the pixels propagated uncertainty when determining regressions.

The function generator introduced error in frequencies that were extremely low or extremely high. At low frequencies, an increase of frequency led to a large increase in amplitude, and at high frequencies the function was irregular and was not as smooth as the intended sinusoidal function. Nevertheless, the use of low and high frequencies was rare.

VII Conclusion

The properties of alternating currents used in modern circuits were analyzed in this lab. The Lissajous figures constructed for RC circuits yielded phase shifts closely matching results from established theory with residual values of less than 1%. The expected natural frequency of the CLR circuit produced a residual of only 7% compared to the value obtained by regression. The transformer yielded an increase in potential before the sudden drop when the frequency surpassed 29 kHz that was explained with hysterics. The magnetic field of a solenoid was analyzed, and a regression was effected, yielding constants with residuals ranging from 0.5% to 28.7%. Finally, a simulation was constructed using the values obtained from the fourth experiment and the magnetic field of two angled solenoids was simulated.

VIII Sources

van Bemmel, H., "AP Physics C Laboratory Manual," DRMO Press, 2019

Cutnell, John D., and Kenneth W. Johnson. Physics. Vol. 5 John Wiley, 2001

Walker, J. et al (2010). Fundamentals of Physics (9th ed.). John Wiley & Sons, Inc.